Journal of Advanced Research in
Numerical Heat Transfer

Journal homepage:
https://semarakilmu.com.my/journals/index.php/arnht/index
ISSN: 2735-0142

Dual Solutions of Two-Dimensional Hybrid Nanofluid Flow and Heat Transfer Past a Porous Medium Permeable Shrinking Sheet with Influence of Heat Generation/Absorption and Convective Boundary Condition

Adnan Asghar[1,3], Mallika Vasugi Govindarajoo[2,*], Khairy Zaimi[3], Haslinda Ibrahim[1], Liaquat Ali Lund[4]

1 School of Quantitative Sciences, UUM College of Arts & Sciences, Universiti Utara Malaysia, 06010 UUM Sintok, Kedah Darul Aman, Malaysia
2 Department of Language and Communications, Faculty of Education and Humanities, UNITAR International University, Petaling Jaya 47301, Malaysia
3 Centre of Excellence for Social Innovation and Sustainability (CoESIS), Institute of Engineering Mathematics, Universiti Malaysia Perlis, Pauh Putra Campus, 02600 Arau, Perlis, Malaysia
4 KCAET Khairpur Mir's, Sindh Agriculture University, Tandojam Sindh 70060, Pakistan

ARTICLE INFO

Article history:
Received 19 August 2024
Received in revised form 18 September 2024
Accepted 18 October 2024
Available online 30 November 2024

Keywords:
Two Dimensional; Dual Solutions; Heat Transfer; Permeable Shrinking Sheet; Porous Medium; Hybrid Nanofluid

ABSTRACT

In this study, the dual solutions of two-dimensional hybrid nanofluid flow and heat transfer past a porous medium permeable shrinking sheet, with the influence of heat generation/absorption and convective boundary conditions, were examined using the bvp4c solver within the MATLAB computational framework. The use of two-dimensional hybrid nanofluid flow and heat transfer in conjunction with a porous medium permeable shrinking sheet, considering the effects of heat generation/absorption and convective boundary conditions, has broad applications in industries such as cooling systems, aerospace, chemical engineering, biomedical applications, energy systems, microfluidics, automotive thermal management, industrial drying, and nuclear reactor cooling. These applications leverage the improved thermal characteristics of hybrid nanofluids and the efficient heat control provided by porous media and convective boundary conditions. The governing partial differential equations (PDEs) are transformed into a system of higher-order ordinary differential equations (ODEs) with their corresponding boundary conditions. These equations are then presented both numerically and graphically. The main objective of this study is to examine the relationship between the solid volume fraction of copper and the permeability parameter of the porous medium, specifically focusing on the values $f''(0)$, and $-\theta'(0)$, in relation to the suction effect. The research also integrates the temperature and velocity profiles of hybrid nanofluid flow, reflecting the influence of porous medium permeability, heat generation/absorption, and convective boundary conditions. Dual solutions are obtained for specific parameter combinations, while non-unique solutions emerge when the critical point reaches $S \geq S_{ci}$ for suction effects. An increase in the intensity of heat generation/absorption and convective boundary conditions leads to a more pronounced temperature profile and a thicker boundary layer. The heat transfer rate $-\theta'(0)$ reduced as the amount of solid volume fraction φ_{Cu} and porous medium permeability parameter P enhanced.

* *Corresponding author.*
E-mail address: mallika@unitar.my (Mallika Vasugi Govindarajoo)

https://doi.org/10.37934/arnht.26.1.6783

1. Introduction

The boundary layer is important because it determines the flow behavior near solid surfaces, has an effect on the drag and lift powers, has an effect on thermal management and heat transfer, offers insights into turbulent flows, and makes it possible to regulate and optimize fluid flow systems [1]. Sakiadis [2] was the first person to propose the idea of a stable two-dimensional boundary layer on a stretched plane. This was initially a novel concept. Crane [3] applied Sakiadis' ideas to flow on two-dimensional linear stretching surfaces and exponential profiles, which allowed for further development and expansion of Sakiadis' research. Over the duration of the last several decades, researchers from a wide range of fields have committed their efforts to developing the development of increased energy exchange fluids. Enhancing the effectiveness of heat transmission has been the major focus of this endeavor. A hybrid nanofluid, which is a novel type of nanofluid, has come into existence as a consequence of this discovery. In contrast to typical nanofluids, which are made up of individual nanoparticles, a hybrid nanofluid is made up of a mixture of many different types of nanoparticles (Devi and Devi [4]). Sajjad *et al.,* [5] state that hybrid nanofluids offer notable benefits and are commonly used in a range of heat transfer applications, including heating plate changers, warmth lines, pipe-formed heat exchangers, and minimal channel radiators. Devi and Devi [6] utilized a hybrid nanofluid consisting of aluminum oxide and copper in their research. The objective was to investigate the effect of two-dimensional stretch surfaces on improving the rate of heat transmission. They successfully found that the thermal conductivity of hybrid nanofluids is significantly greater than that of ordinary fluids, resulting in a more efficient rate of heat transmission. Lund *et al.,* [7] examined the effects of radiation on a sheet that undergoes both stretching and shrinking, in the presence of unstable magnetohydrodynamic hybrid nanofluid flow. A variety of numerical studies have been carried out to investigate a hybrid nanofluid using different models, with the parameters depending on the specific conditions [8-28].

Various engineering disciplines, such as petroleum and environmental engineering, civil engineering, biological engineering, agriculture, and others, rely significantly on the modelling of fluid flow and thermal transfer in porous media. The thermal transportation of a chemically reactive flow of magnetized hybrid nanofluids over a Darcian porous media was investigated by Waqas *et al.,* [29]. Venkateswarlu *et al.,* [30] studied the entropy-optimized flow of convective trihybrid nanofluid with temperature-dependent viscosity in a porous media. Nazir *et al.,* [31] looked on the non-Fourier thermal and solute transit of Williamson hybrid nanofluid in porous media. Oudina *et al.,* [32] conducted a study on the role of porous media and magneto-convective flow in Hybrid-nanofluid to the creation of entropy. The MHD Williamson hybrid nanofluid flow with ohmic heating in a porous medium and convective boundary condition was examined by Rashad *et al.,* [33]. The more studies on porous media and different physical models that have been conducted recently are shown in refs. [34-39].

These are the limitations that must be met at the borders of a physical system, such as a solid, a fluid, or an electromagnetic field. Boundary requirements are also known as boundary conditions. The behaviour of the system and the way it interacts with its environment are both significantly influenced by these variables, which play a very important role. In a physical sense, boundary conditions can be considered to represent the particular circumstances that are present at the borders of various materials or areas of space. For instance, when we take into consideration the behaviour of a fluid that is flowing through a pipe, the boundary conditions at the walls of the pipe may define the velocity or pressure of the fluid at those locations, or they may specify that the fluid is unable to penetrate the wall or surface. Convective boundary conditions discover practical uses in the nuclear power plants, oxygenation, hemodialysis, laser therapy, sanitary fluid transportation, gas turbines, and material drying (Sayed *et al.,* [40]). Convective boundary conditions were initially reported to be used by Aziz [41] in his analysis of the Blasius flow. Aly and Pop [42] used suction and convective boundaries to study the Two-dimensional across a stretch and shrinking sheet. The convective rotational flow hybrid nanofluid over the linear stretching/shrinking sheet was investigated by Asghar *et al.,* [43]. Further, Khashi *et al.,* [44] investigated the stretching/shrinking layer that is passed by a steady hybrid nanofluid flow under convective boundary and velocity slip circumstances. Yahaya *et al.,* [45] conducted research on the MHD hybrid nanofluid that was caused by a radially decreasing disk stagnation point flow with a convective boundary condition for dual solutions. Waini *et al.,* [46] examined the convective boundary condition regarding hybrid nanofluid flow and heat transfer past a permeable stretching/shrinking surface. Further research has also investigated the effects of the convective boundary condition in hybrid nanofluids using various consideration models in [47-49].

When it comes to managing heat transfer, heat generation and heat absorption are also among the most important components. The occurrence of heat generation and heat absorption, as well as their effects, are important to understand for a variety of industrial processes, including the cooling of nuclear power plants, hydrothermal sources, and energy absorption, amongst others. Hayat and Nadeem [50] investigated the steady flow hybrid nanofluid in the context of the presence of heat energy absorption and generation, radiation, and chemical activities. Zainal *et al.,* [51] investigated a hybrid nanofluid, focusing on the effects of heat generation and heat absorption on the bidirectionally stretched and shrinking layer. In addition, Wahid *et al.,* [52] conducted research in two dimensions to explore the constant flow across an exponentially stretched and shrinking permeability, as well as the heat source effect under the slip conditions. Recently, a study conducted by Ahmad *et al.,* [53] investigated the transfer of mass and energy in a hybrid nanofluid flow across a spinning sphere, considering the effects of heat generation/absorption and magnetic field. Heat generation/absorption have been the subject of a different model of study in [54-56].

According to the study survey that was mentioned before, the rheological properties and heat transfer characteristics of hybrid nanofluids are of significant value in engineering applications. Consequently, the main objective of this inquiry is to explore the behaviour of the solid volume fraction copper and porous medium permeability parameter for $f''(0)$ and $-\theta'(0)$ in response to the suction effect. In addition, this study has also incorporated the temperature and velocity profile of a hybrid nanofluid flow, which corresponds to the effect of porous medium permeability, heat generation/absorption, and convective boundary condition. This was done in order to better understand the relationship between these dynamics. The computational outcomes of this effort are contrasted to the outcomes of earlier scholarly investigations. The findings of this study have not been explored or published by any other researcher, as far as the author is aware. This is what makes the novel conceivable, according to the author's best knowledge.

2. Methodology

2.1 Mathematical Model and Formulation

Figure 1 is a demonstration of the steady flow two dimensional past a porous medium permeable shrinking sheet with heat generation/absorption that appears in hybrid nanofluids. In a coordinate system where the x and y axes are Cartesian coordinates, the sheet is measured together with the x axis, the y axis is normal to it, and the complete coordinate system is the sheet that is positioned at $y = 0$. The surface is assumed to be shrinking at a velocity of $u_w(x) = bx$, where b is a constant and v_w is the wall mass flow velocity. It is probable that a hot fluid with a uniform temperature of T_f, which provides a heat transfer coefficient of h_f, heats the plate's bottom surface by convection. The temperature at the surface T_w, and the ambient fluid temperature T_∞ is the product of a convection heating process, we have $T_f > T_w > T_\infty$. There is a water base copper alumina hybrid nanofluid that is taken into consideration here. In this case, the size of the nanoparticles is assumed to be uniform, and the effects of nanoparticle agglomeration on thermophysical characteristics are disregarded. This is because the nanofluid is produced from the nanoparticles and the base fluid as a stable combination. In addition, heat generation/absorption are taken into consideration.

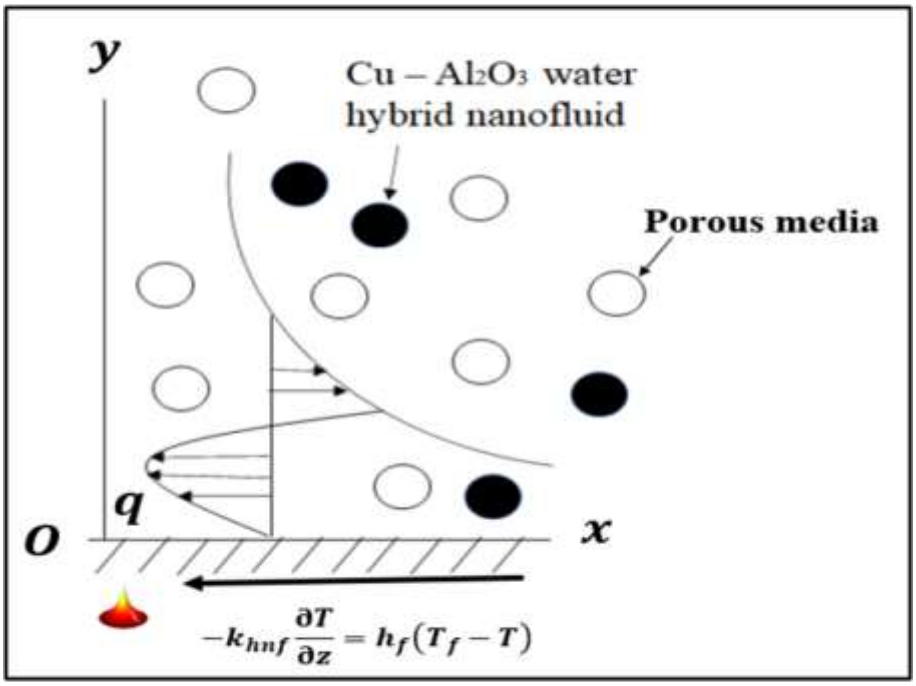

Fig.1. The physical geomerty and coordinate system

The governing equations for continuity, momentum, and energy of a hybrid nanofluid are formulated as follows, taking into account the assumptions that have been made (Devi and Devi [6]; Waini *et al.,* [46]):

$$u_x + v_y = 0, \quad (1)$$

$$uu_x + vu_y = \frac{\mu_{hnf}}{\rho_{hnf}}u_{yy} - \frac{\mu_{hnf}}{\rho_{hnf}K_p}u, \quad (2)$$

$$uT_x + vT_y = \frac{k_{hnf}}{(\rho c_p)_{hnf}}T_{yy} + \frac{q}{(\rho c_p)_{hnf}}(T - T_\infty). \quad (3)$$

The associated the boundary conditions (Waini *et al.,* [46]):

$$v = v_w(x),\ u = u_w,\ -k_{hnf}T_y = h_f(T_f - T)\ \text{as}\ y = 0, \quad (4)$$
$$u \to 0,\ T \to T_\infty \quad \text{as}\ y \to \infty.$$

The components of the velocities are denoted by the letters u and v, respectively, when considering the hybrid nanofluid along the x and y axis. The temperature of the hybrid nanofluid is denoted by the letter T. Moreover, $v_w(x) = -\sqrt{b\nu_f}\,S$ where $f(0) = S$ is the mass flux velocity parameter, while S signifies the suction $S > 0$, and when $S < 0$ injection parameter. The base fluid kinematic viscosity is represented by ν_f.

In addition, μ_{hnf} is corresponded to by dynamic viscosity, ρ_{hnf} shows the density, k_{hnf} is equivalent to the thermal conductivity, and $(\rho c_p)_{hnf}$ describes the heat capacity of the hybrid nanofluid. The subscripts f, nf, hnf, Al_2O_3, and Cu denote base fluid, nanofluid, hybrid nanofluid, $S1$ solid nanoparticle 1, and $S2$ solid nanoparticle 2. The thermophysical properties of copper, alumina, and water nanoparticles are shown in Table 1. Table 2 displays the hybrid nanofluid's thermophysical properties.

Table 1
The thermophysical properties of copper, alumina and water nanoparticles (Waini *et al.,* [46])

	Pr	k (W/mK)	c_p (J/kgK)	ρ (kg/m^3)
Copper (Cu)	-	400	385	8933
Alumina (Al_2O_3)	-	40	765	3970
Water (H_2O)	6.2	0.613	4179	997.1

Table 2
Thermophysical properties of hybrid nanofluid (Waini *et al.,* [46])

Names	Properties
Dynamic viscosity	$\mu_{hnf} = \dfrac{\mu_f}{(1-\varphi_{Cu})^{5/2}(1-\varphi_{Al_2O_3})^{5/2}}$
Density	$\rho_{hnf} = (1-\varphi_{Cu})\left[(1-\varphi_{Al_2O_3})\rho_f + \varphi_{Al_2O_3}\rho_{Al_2O_3}\right] + \varphi_{Cu}\rho_{Cu}$
Thermal conductivity	$k_{hnf} = \frac{k_{Cu}+2k_{nf}-2\varphi_{Cu}(k_{nf}-k_{Cu})}{k_{Cu}+2k_{nf}+\varphi_{Cu}(k_{nf}-k_{Cu})} \times (k_{nf})$, where $k_{nf} = \frac{k_{Al_2O_3}+2k_f-2\varphi_{Al_2O_3}(k_f-k_{Al_2O_3})}{k_{Al_2O_3}+2k_f+\varphi_{Al_2O_3}(k_f-k_{Al_2O_3})} \times (k_f)$
Heat capacity	$(\rho c_p)_{hnf} = (1-\varphi_{Cu})\left[(1-\varphi_{Al_2O_3})(\rho c_p)_f + \varphi_{Al_2O_3}(\rho c_p)_{Al_2O_3}\right] + \varphi_{Cu}(\rho c_p)_{Cu}$

The similarity variables in this instance are explained below (Waini *et al.,* [46]).

$$u = bxf'(\eta), \quad v = -\sqrt{b\nu_f}f(\eta), \quad \theta(\eta) = \frac{T-T_\infty}{T_f-T_\infty}, \quad \eta = y\sqrt{\frac{b}{\nu_f}}, \tag{5}$$

Eq. (1) is completely satisfied. Eqs. (2)-(3) have been transformed into ordinary differential equations, together with the boundary conditions from Eq. (4), using the similarity variables defined in Eq. (5).

$$\frac{\mu_{hnf}/\mu_f}{\rho_{hnf}/\rho_f}f''' + f''f - (f')^2 - \frac{\mu_{hnf}/\mu_f}{\rho_{hnf}/\rho_f}Pf' = 0, \tag{6}$$

$$\frac{1}{Pr(\rho c_p)_{hnf}/(\rho c_p)_f}\left[k_{hnf}/k_f\right]\theta'' + \theta' f + \frac{1}{(\rho c_p)_{hnf}/(\rho c_p)_f}Q\theta = 0. \tag{7}$$

transformed boundaries condition,

$$f(0) = S, \quad f'(0) = -1, \quad -k_{hnf}/k_f\,\theta'(0) = Bi[1-\theta(0)], \tag{8}$$
$$f'(\eta) \to 0, \ \theta(\eta) \to 0 \ \text{at} \ \eta \to \infty.$$

Additionally, $P=\frac{\nu_f}{bK_p}$ denotes the porous medium permeability parameter, $Pr=\frac{(\mu c_p)_f}{k_f}$ is Prandtl member, $Q=\frac{q}{b(\rho c_p)_f}$ shows heat generation/absorption, and $Bi=\frac{h_f}{k_f}\sqrt{\frac{\nu_f}{b}}$ represents the Biot number.

The skin friction coefficient c_f and local Nusselt number Nu_x are significant physical quantities that are expressed as.

$$c_f=\frac{\mu_{hnf}}{u_w^2\rho_f}\left(u_y\right)_{y=0},\ Nu_x=\frac{x}{(T_f-T_\infty)k_f}\left[-k_{hnf}\left(T_y\right)_{y=0}\right], \tag{9}$$

By employing Eqs. (5) and (9) and the resulting terms obtained

$$(Re_x)^{0.5}c_f=\frac{\mu_{hnf}}{\mu_f}f''(0),\ \ (Re_x)^{-0.5}Nu_x=-\left[\frac{k_{hnf}}{k_f}\right]\theta'(0), \tag{10}$$

where $Re_x=\frac{x\,u_w(x)}{\nu_f}$ expressed as the local Reynolds number.

2.2 Numerical Method

To numerically solve the system of higher-order nonlinear ODEs shown in Eqs. (6)-(7) with the boundary conditions shown in Eq. (8), the bvp4c solver is used. This solver runs on the MATLAB program. For the purpose of providing fourth-order numerical solutions, the bvp4c approach is a finite difference system that uses the three-stage Lobatto IIIA implicit Runge–Kutta technique. The following phases of the numerical method are below:

Phase 1: New variables are inserted into the framework of higher-order nonlinear ODEs in Eqs. (6)-(7):

$$y(1)=f,y(2)=f',y(3)=f'',y(4)=\theta,y(5)=\theta'. \tag{11}$$

Phase 2: Using the new variables in Eq. (11), transform the system of higher-order nonlinear ODEs in Eqs. (6)-(7) into a system of first order nonlinear ODEs:

$$\begin{aligned}
&f'=y(2),\\
&f''=y(3),\\
&f'''=\frac{\rho_{hnf}/\rho_f}{\mu_{hnf}/\mu_f}\left(\left(y(2)\right)^2-y(1)y(3)+\frac{\mu_{hnf}/\mu_f}{\rho_{hnf}/\rho_f}Py(2)\right),\\
&\theta'=y(5),\\
&\theta''=\frac{Pr(\rho c_p)_{hnf}/(\rho c_p)_f}{(k_{hnf}/k_f)}\left(-y(1)y(5)-\frac{1}{(\rho c_p)_{hnf}/(\rho c_p)_f}Qy(4)\right).
\end{aligned} \tag{12}$$

Phase 3: To express the boundary conditions (8) in terms of the additional variables in Eq. (11):

$$y(1)_a=S,y(2)_a=-1\ ,-\frac{k_{hnf}}{k_f}y(5)_a=Bi[1-y(4)_a],y(2)_b=0,y(4)_b=0. \tag{13}$$

It is important that the subscript $'a'$ shows the position of the surface for $\eta = 0$, whereas the subscript $'b'$ denotes the location away from the surface for a certain η. In this study, the location is set to $\eta = 8$.

Phase 4: To get dual solutions, provide the bvp4c solver with two separate starting estimates one at a time. The first solution can be found using less restricted starting assumptions, but this is not necessarily true for the second solution. This method is repeated until the numerical solutions asymptotically meet the boundary conditions at infinity (Eq. (8)).

3. Results

The solutions duality depicted in the graphs was accomplished by employing a range of initial guesses for $f''(0)$, and $-\theta'(0)$. Consequently, the velocity and temperature profiles were able to satisfy the boundary condition $\eta \to \infty$ in an asymptotically satisfying manner. To make sure that the method is accurate, the results that are currently being used are validated by utilizing data from earlier studies. Table 3 presents a comparison for values of $f''(0)$ under different parameters, including $\varphi_{Al_2O_3} = \varphi_{Cu} = P = Q = B = 0$, $Pr = 0.7$, and $S = 3$. These results are compared with the findings of Waini *et al.*, [57], and Ghosh and Mukhopadhyay [58]. These findings are presented in Table 3, which show that there is a remarkable consistency between them.

Table 3
Comparison values of $f''(0)$ with various parameters $\varphi_{Al_2O_3} = \varphi_{Cu} = P = Q = B = 0$, $Pr = 0.7$, and $S = 3$

	First solution $f''(0)$	Second solution $f''(0)$
Waini *et al.,* [57]	2.39081	−0.97224
Ghosh and Mukhopadhyay [58]	2.39082	−0.97223
Existing Study	2.3907156	−0.9723215

The reduced skin friction $f''(0)$ and reduced heat transfer $-\theta'(0)$ are presented in Figures 2-5. Figures 2-3 shows the $f''(0)$, and $-\theta'(0)$ against suction effect with various values of specific parameters such as $\varphi_{Al_2O_3} = 0.1, Pr = 6.2, Q = P = Bi = 1.0$ for different solid volume fraction $\varphi_{Cu} = 0.01, 0.03$, and 0.05 in which velocity and temperature profiles were able to satisfy the boundary condition $\eta \to \infty$ in an asymptotically satisfying manner. Dual solutions meet at critical points where the first and second solution connect with each other. Beyond the critical points no solutions are obtained. The critical points $S_{c1} = 1.5001, S_{c2} = 1.4991$, and $S_{c3} = 1.4850$ attained correspond to $\varphi_{Cu} = 0.01, 0.03$, and 0.05 respectively. From Figure 2, $f''(0)$ augmented in first solution but declined in second solution as enhanced the quantity of φ_{Cu}. Solid particles copper, in the fluid can affect the momentum transfer characteristics near the wall. Solid particles interrupt the boundary layer flow, altering the velocity gradient at the wall. This can lead to a reduction in the fluid's shear stress on the surface and decreased skin friction. From Figure 3, $-\theta'(0)$ declined in both solutions as the quantity of φ_{Cu} heightened. Copper has a higher heat conductivity than most fluids. When copper particles are introduced into the fluid, the total thermal conductivity of the combination rises. While this may appear contradictory, an increase in thermal conductivity can cause a decrease in the temperature gradient near the wall, lowering the driving force for convective heat transfer $-\theta'(0)$. In addition, when copper particles are introduced in high amounts, they may cluster together, creating agglomerates. These agglomerates may form zones with low effective thermal conductivity, resulting in low heat transport in those locations. Clustering affects the regular distribution of copper, which is required for efficient heat conduction.

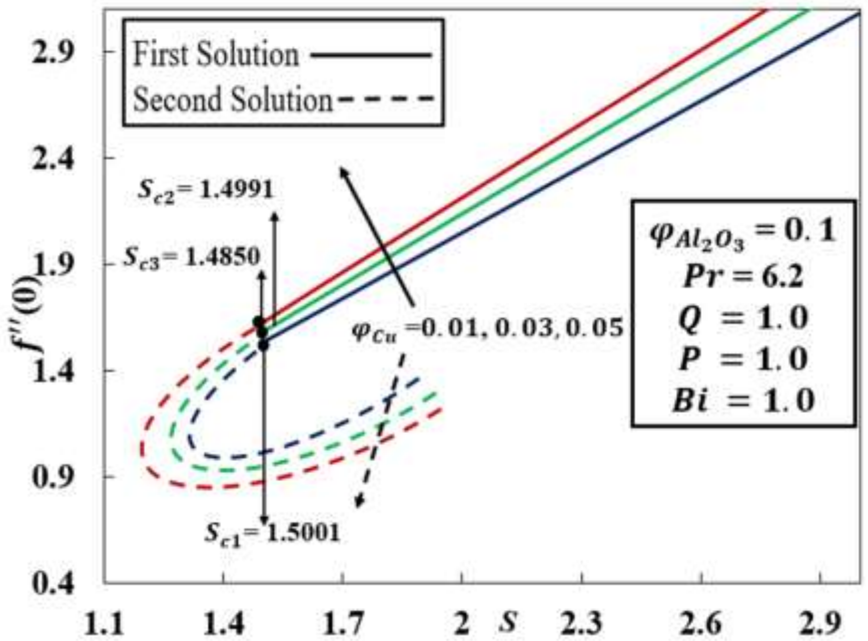

Fig. 2. Variation of $f''(0)$ against suction S effect for different values of φ_{Cu}

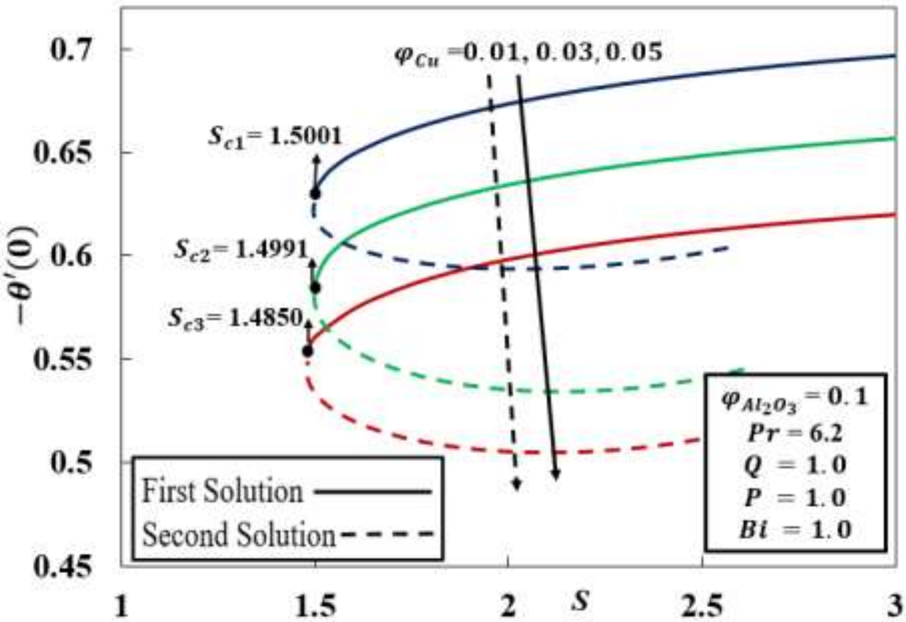

Fig. 3. Variation of $-\theta'(0)$ against suction S for different values of φ_{Cu}

Figures 4-5 display the $f''(0)$, and $-\theta'(0)$ in relation to the suction effect for different values of specific parameters, such as $\varphi_{Al_2O_3} = 0.1, \varphi_{Cu} = 0.01, Pr = 6.2, Q = Bi = 1.0$, for varying porous medium permeability parameter $P = 0.0, 0.5$ and 1.0 with velocity and temperature profiles met the boundary requirement $\eta \to \infty$ an asymptotically acceptable approach. The critical points are $S_{c1} = 1.8051, S_{c2} = 1.5811$, and $S_{c3} = 1.5001$ accomplished relate to $P = 0.0, 0.5$, and 1.0 respectively. Dual solutions are obtained in specific ranges of parameters. From Figure 4, $f''(0)$ boosted in both solutions as higher the quantity of P. The fluid can enter the porous structure more readily as the permeability of the porous medium rises. Higher $f''(0)$ results from the fluid's enhanced contact with the porous medium's solid matrix, which increases the fluid's drag forces. In addition, with intensified permeability, the effective roughness of the surface can appear to increase. This is because the fluid interacts more with the rougher internal surfaces of the porous medium. Increased roughness typically enhances turbulence and shear forces near the wall, contributing to higher $f''(0)$. From Figure 5 , $-\theta'(0)$ declined as the quantity of P improved. Greater heat conduction inside the porous material is made possible by its higher permeability. Although this can enhance heat conduction, it lowers the convective heat transfer coefficient overall by lessening the temperature differential close to the wall. This results in a drop in the $-\theta'(0)$, which gauges convective heat transfer in comparison to conductive heat transfer. Also, the major heat transport mechanism in a highly permeable media might change from convection to conduction inside the porous matrix. This shift affects total convective heat transfer efficiency, resulting in a drop in the $-\theta'(0)$.

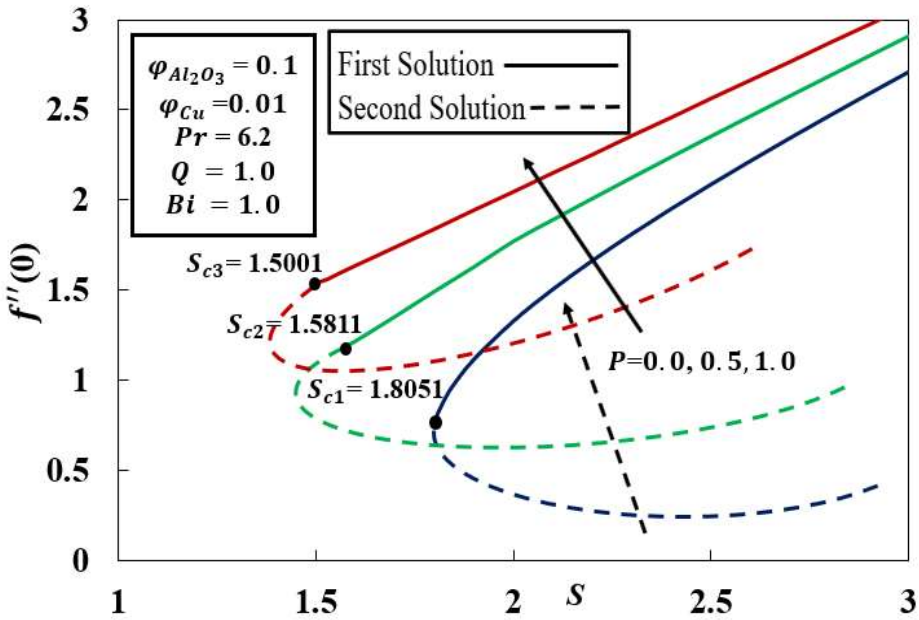

Fig. 4. Variation of $f''(0)$ against suction S for different values of P

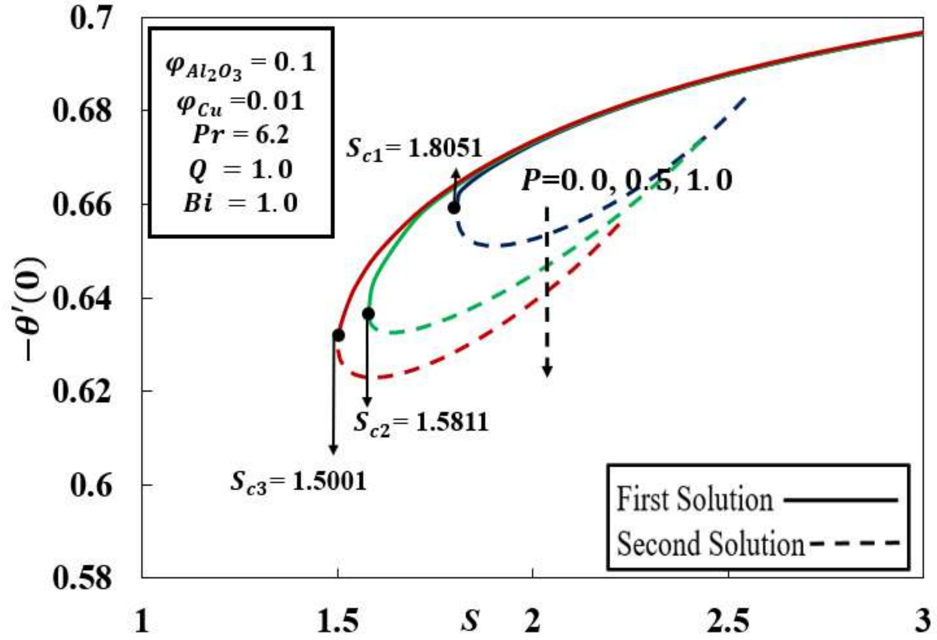

Fig. 5. Variation of $-\theta'(0)$ against suction S for different values of P

Figures 6-7 exhibit the velocity profile $f'(\eta)$, and temperature profile $\theta(\eta)$ with different values of parameters, such as $\varphi_{Al_2O_3} = 0.1, \varphi_{Cu} = 0.01, Pr = 6.2,\ S = 2.5, Q = Bi = 1.0,$ for different porous medium permeability parameter $P = 0.0, 0.5$ and 1.0 in which velocity and temperature profiles met the boundary requirement $\eta \to \infty$ in an asymptotically acceptable approach. In Figure 6, it is noticed that $f'(\eta)$ profile enhanced in first solution and declined in second solution for the higher value of permeability parameter P. Physically, the resistance to fluid movement inside the porous structure reduces as the porous medium's permeability rises. This indicates that instead of flowing over the porous medium's surface, a greater amount of the fluid can permeate and pass through it. This redistribution of flow lowers the fluid's velocity throughout the medium's surface. Furthermore, the boundary layer close to the porous medium's surface may thicken as permeability increases. The fluid velocity falls more gradually from the free stream to the wall in a thicker boundary layer because of its lower velocity gradient. As a result, the velocity profile close to the surface generally decreases. From figure 7, $\theta(\eta)$ profile decreased in both solutions as the value of P increased. The thermal boundary layer close to the porous medium's surface may thicken as permeability increases. A lower overall temperature gradient is the result of a more gradual temperature transition from the wall to the bulk fluid, which is indicated by a thicker thermal boundary layer. Apart from that, increased permeability in the porous material allows for increased heat conduction. Heat may be dispersed throughout the medium more successfully thanks to this enhanced conduction, which lowers the temperature gradient and produces a more uniform temperature profile.

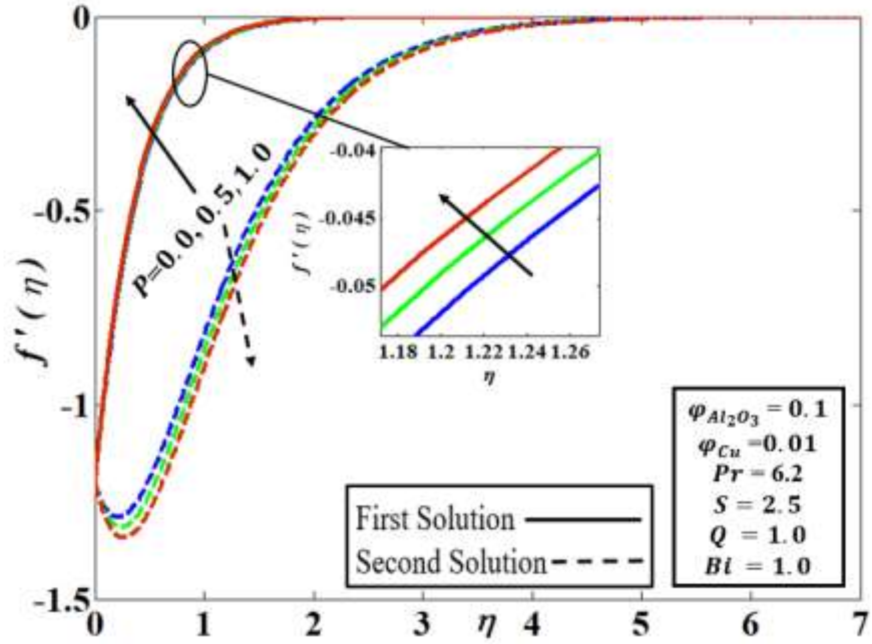

Fig. 6. Velocity profile $f'(\eta)$ for different values of P

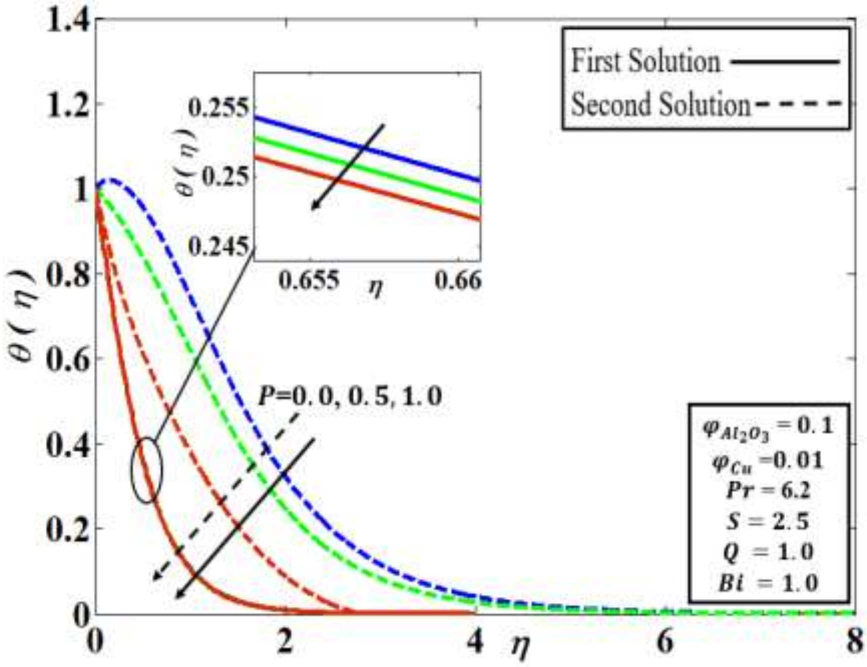

Fig. 7. Temperature profile $\theta(\eta)$ for different values of P

Figures 8 reveal the temperature profile $\theta(\eta)$ with different values of parameters, such as $\varphi_{Al_2O_3} = 0.1$, $\varphi_{Cu} = 0.01$, $Pr = 6.2$, $S = 2.5$, $P = Bi = 1.0$ for different heat generation and absorption parameter $Q = 0.1, 0.5$, and 1.0 where velocity and temperature profiles met the boundary requirement $\eta \to \infty$. From Figure 8, it is observed that both solutions are enhanced if the amount of heat generation/absorption parameter is higher. A greater quantity of thermal energy is delivered directly into the system if there is an increase in the amount of heat production that occurs within the medium. The medium and the fluid that surrounds it both experience an increase in temperature as a result of this increased energy, which ultimately results in a higher temperature profile. In addition, the greater the amount of heat that is generated, the greater the thermal gradient that exists between the heat source and the medium that is around it. Because of this bigger gradient, the rate of heat transfer from the source to the fluid in the surrounding area is increased, which results in an increase in the temperature profile.

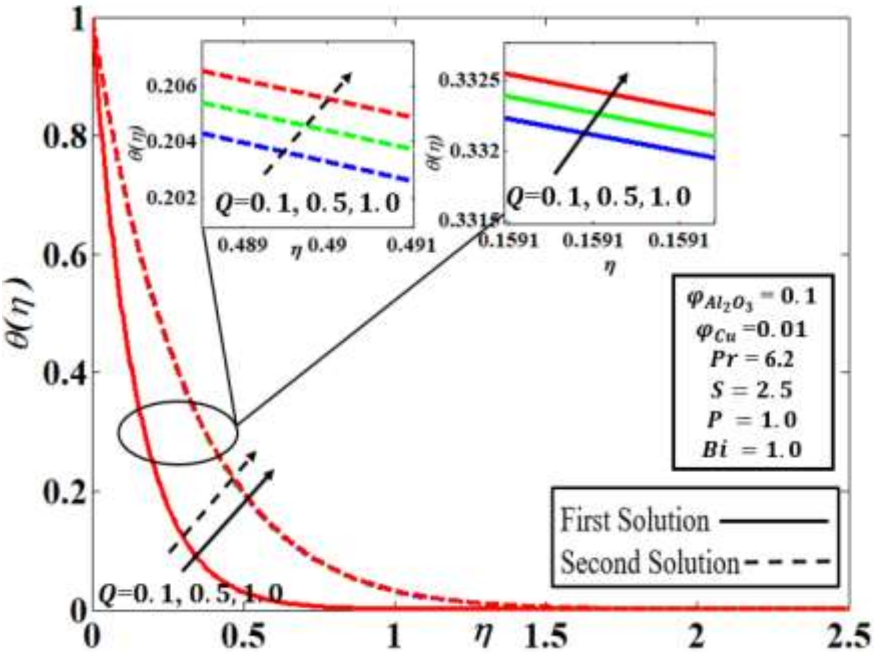

Fig. 8. Temperature profile $\theta(\eta)$ for different values of Q

As shown in Figure 9, the temperature profile $\theta(\eta)$ is revealed with various parameter values, including $\varphi_{Al_2O_3} = 0.1, \varphi_{Cu} = 0.01, Pr = 6.2, S = 2.5, P = Q = 1.0$. These values correspond to distinct convective boundary condition parameters $Bi = 0.1, 0.5$, and 1.0 with velocity and temperature profiles met the boundary requirement $\eta \to \infty$. Figure 9 shows that both solutions improve as the quantity of convective boundary condition increases. Physically, there is an increase in the rate of heat transfer from the surface to the fluid that is around it as the convective boundary condition is enhanced. Because of this, heat is removed from the surface in a more effective manner, which leads to an increase in the temperature of the surface and, as a consequence, an increase in the temperature profile of the fluid layers that are close to it. It is implied that there is a greater heat flow at the border when the convective boundary condition is stronger. Because of this higher flow, the temperature close to the surface rises, which results in a more pronounced temperature gradient between the surface and the fluid. Because of this larger gradient, more heat is absorbed by the fluid, which results in an increase in the temperature profile as a whole. Further enhancing the convective conditions inside the fluid allows for a more efficient redistribution of energy throughout the fluid. This rearrangement guarantees that heat from the surface is distributed more effectively throughout the fluid, which results in an increase in the temperature profile in places that could have been colder under circumstances of weaker convection.

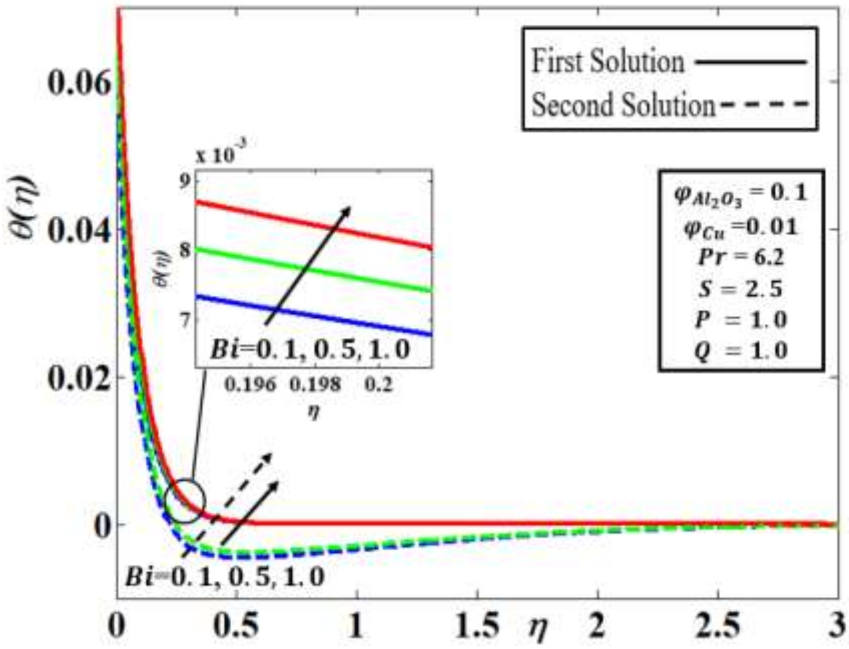

Fig. 9. Temperature profile $\theta(\eta)$ for different values of Bi

4. Conclusions

In this investigation, the bvp4c solver, in combination with the MATLAB computational framework, was employed to examine the dual solutions of two-dimensional hybrid nanofluid flow and heat transfer past a porous medium permeable shrinking sheet, influenced by heat generation/absorption and convective boundary conditions. To demonstrate the accuracy of the modeling method discussed in this work, the coding implemented with the bvp4c algorithm was thoroughly evaluated. The governing partial differential equations (PDEs) are transformed into a set of higher-order ordinary differential equations (ODEs) with their corresponding boundary conditions, which are then presented both numerically and graphically. The primary goal of this study is to investigate the behavior of the solid volume fraction of copper and the porous medium permeability parameter for $f''(0)$, and $-\theta'(0)$ in response to the suction effect. The current investigation also incorporates the temperature and velocity profiles of hybrid nanofluid flow, which are correlated with the influence of porous medium permeability, heat generation/absorption, and convective boundary conditions. Dual solutions are obtained for specific combinations of parameters. Hybrid nanofluid flows exhibit a unique solution up to a critical point $S < S_{ci}$ for suction effects. The temperature profile and boundary layer thickness increase with the intensification of heat generation/absorption and convective boundary conditions.

Hybrid nanofluids, composed of a combination of various nanoparticles, are used to enhance the thermal conductivity and heat transfer capabilities of the base fluid. This approach is particularly beneficial in cooling systems for electronic equipment, where efficient heat dissipation is crucial for maintaining performance and preventing overheating. Controlling the rate of heat transfer is also critical in industries where drying processes are essential, such as food processing and textiles. The optimization of these processes can be achieved through the use of hybrid nanofluids and porous media, leading to improved product quality and uniform drying. The study could be expanded to three-dimensional flows, which are more representative of practical engineering systems. This would provide a more detailed understanding of the flow and heat transfer mechanisms in complex geometries. Future research could focus on optimizing the parameters involved, such as the solid volume fraction of nanoparticles, permeability of the porous medium, and the heat generation/absorption rate, to achieve desired heat transfer characteristics for specific applications. The study can be extended to investigate the effects of various hybrid nanofluid combinations, including different types, sizes, and concentrations of nanoparticles.

Acknowledgement

"This research was not funded by any grant"

References

[1] *Boundary layer theory*. McGraw-Hill Book Company, 1968.
[2] Sakiadis, Byron C. "Boundary-layer behavior on continuous solid surfaces: I. Boundary-layer equations for two-dimensional and axisymmetric flow." *AIChE Journal* 7, no. 1 (1961): 26-28. https://doi.org/10.1002/aic.690070108
[3] Sakiadis, Byron C. "Boundary-layer behavior on continuous solid surfaces: I. Boundary-layer equations for two-dimensional and axisymmetric flow." *AIChE Journal* 7, no. 1 (1961): 26-28. https://doi.org/10.1002/aic.690070108
[4] Devi, SP Anjali, and S. Suriya Uma Devi. "Numerical investigation of hydromagnetic hybrid Cu–Al2O3/water nanofluid flow over a permeable stretching sheet with suction." *International Journal of Nonlinear Sciences and Numerical Simulation* 17, no. 5 (2016): 249-257. https://doi.org/10.1515/ijnsns-2016-0037
[5] Sajjad, Muhammad, Ali Mujtaba, Adnan Asghar, and Teh Yuan Ying. "Dual solutions of magnetohydrodynamics Al2O3+ Cu hybrid nanofluid over a vertical exponentially shrinking sheet by presences of joule heating and thermal slip condition." *CFD Letters* 14, no. 8 (2022): 100-115. https://doi.org/10.37934/cfdl.14.8.100115
[6] Devi, S. U., & Devi, S. A. (2017). Heat transfer enhancement of cu− $ al_ {2} o_ {3} $/water hybrid nanofluid flow over a stretching sheet. *Journal of the Nigerian Mathematical Society*, *36*(2), 419-433.
[7] Lund, Liaquat Ali, Zurni Omar, Ilyas Khan, and El-Sayed M. Sherif. "Dual solutions and stability analysis of a hybrid nanofluid over a stretching/shrinking sheet executing MHD flow." *Symmetry* 12, no. 2 (2020): 276. https://doi.org/10.3390/sym12020276
[8] Sakkaravarthi, K., and Bala Anki Reddy P. "Entropy generation on MHD flow of Williamson hybrid nanofluid over a permeable curved stretching/shrinking sheet with various radiations." *Numerical Heat Transfer, Part B: Fundamentals* 85, no. 3 (2024): 231-257. https://doi.org/10.1080/10407790.2023.2231633
[9] Shah, Zahir, Adnan Asghar, Teh Yuan Ying, Liaquat Ali Lund, Ahmed Alshehri, and Narcisa Vrinceanu. "Numerical investigation of sodium alginate-alumina/copper radiative hybrid nanofluid flow over a power law stretching/shrinking sheet with suction effect: a study of dual solutions." *Results in Engineering* 21 (2024): 101881. https://doi.org/10.1016/j.rineng.2024.101881
[10] Ahmed, A., S. Muhammad, and M. A. T. Ucheri. "Hybrid Nano Fluid Slip Flow Over a Permeable Sheet with Radiative Heat Flux, Variable Thermal Conductivity and Heat Source." *Physical Science International Journal* 28, no. 4 (2024): 86-101. https://doi.org/10.9734/psij/2024/v28i4840
[11] Asghar, Adnan, Abdul Fattah Chandio, Zahir Shah, Narcisa Vrinceanu, Wejdan Deebani, Meshal Shutaywi, and Liaquat Ali Lund. "Magnetized mixed convection hybrid nanofluid with effect of heat generation/absorption and velocity slip condition." *Heliyon* 9, no. 2 (2023). https://doi.org/10.1016/j.heliyon.2023.e13189
[12] Sachhin, S. M., U. S. Mahabaleshwar, H. N. Huang, B. Sunden, and Dia Zeidan. "An influence of temperature jump and Navier's slip-on hybrid nano fluid flow over a permeable stretching/shrinking sheet with heat transfer and inclined MHD." *Nanotechnology* 35, no. 11 (2023): 115401. https://doi.org/10.1088/1361-6528/ad13be
[13] Kalyan, Shreedevi, Ashwini Sharan, and Ali J. Chamkha. "Heat and mass transfer of two immiscible flows of Jeffrey fluid in a vertical channel." *Heat Transfer* 52, no. 1 (2023): 267-288. https://doi.org/10.1002/htj.22694
[14] Saraswathi, H., and K. Shreedevi Kalyan. "Steady Jeffery Fluid through Porous Media in Presence of a Baffle in a Vertical Channel." *Journal of Nanofluids* 12, no. 6 (2023): 1644-1651. https://doi.org/10.1166/jon.2023.2047
[15] Kalyan, Shreedevi. "Numerical study of electrically conducting MHD fluids in a vertical channel with Jeffrey fluid flow and first order chemical reaction." *Thermal Science and Engineering* 6, no. 2 (2023): 3968. https://doi.org/10.24294/tse.v6i2.3968
[16] Soliman, Hussein Abd Allah. "Analysis of Micropolar Immiscible Fluid Flow on Electrically Conducting Free Convective Flow in a Vertical Channel in the Presence of Chemical Reaction." *International Journal of Advanced Engineering and Business Sciences* 5, no. 1 (2024). https://doi.org/10.21608/ijaebs.2024.273140.1093
[17] Madhu, Shreedevi Kalyan, Yamanappa Gudagi, Varun Kumar, Raman Kumar, and Sureshkumar. "Fluid Sustainability by the Effect of Microrotational Flow and Chemical Reactions in a Vertical Channel." *International Journal of Modelling and Simulation*, (2024): 1–12. https://doi.org/10.1080/02286203.2024.2319008

[18] Bakar, Shahirah Abu, Norihan Md Arifin, and Ioan Pop. "Stability analysis on mixed convection nanofluid flow in a permeable porous medium with radiation and internal heat generation." *Journal of Advanced Research in Micro and Nano Engineering* 13, no. 1 (2023): 1-17. https://doi.org/10.37934/armne.13.1.117
[19] Teh, Yuan Ying, and Adnan Ashgar. "Three dimensional MHD hybrid nanofluid Flow with rotating stretching/shrinking sheet and Joule heating." *CFD Letters* 13, no. 8 (2021): 1-19. https://doi.org/10.37934/cfdl.13.8.119
[20] Asghar, Adnan, Teh Yuan Ying, and Wan Mohd Khairy Adly Wan Zaimi. "Two-dimensional mixed convection and radiative Al2O3-Cu/H2O hybrid nanofluid flow over a vertical exponentially shrinking sheet with partial slip conditions." *CFD Letters* 14, no. 3 (2022): 22-38. https://doi.org/10.37934/cfdl.14.3.2238
[21] Ramanuja, M., Kavitha, J., Sudhakar, A., Babu, A. A., Sree, H. K., & Babu, K. R. (2023). Effect of Chemically Reactive Nanofluid Flowing Across Horizontal Cylinder: Numerical Solution. *Journal of Advanced Research in Numerical Heat Transfer*, 12(1), 1-17.
[22] Asghar, Adnan, Teh Yuan Ying, and Khairy Zaimi. "Two-dimensional magnetized mixed convection hybrid nanofluid over a vertical exponentially shrinking sheet by thermal radiation, joule heating, velocity and thermal slip conditions." *Journal of Advanced Research in Fluid Mechanics and Thermal Sciences* 95, no. 2 (2022): 159-179. https://doi.org/10.37934/arfmts.95.2.159179
[23] Loon, Yew Wai, and Nor Azwadi Che Sidik. "A comprehensive review of recent progress of nanofluid in engineering application: Microchannel heat sink (MCHS)." *Journal of Advanced Research in Applied Sciences and Engineering Technology* 28, no. 2 (2022): 1-25. https://doi.org/10.37934/araset.28.2.125
[24] Baithalu, Rupa, and S. R. Mishra. "On the free convection of magneto-micropolar fluid in association with thermal radiation and chemical reaction and optimized heat transfer rate using response surface methodology." *Modern Physics Letters B* 37, no. 33 (2023): 2350171. https://doi.org/10.1142/S0217984923501713
[25] Baithalu, Rupa, S. R. Mishra, and Subhajit Panda. "Magnetic dissipation on radiative free convection of a conducting hybrid nanofluid within a rotating cone and circular disc." *Partial Differential Equations in Applied Mathematics* 11 (2024): 100788. https://doi.org/10.1016/j.padiff.2024.100788
[26] Panda, Subhajit, Rupa Baithalu, S. Baag, and S. R. Mishra. "Behaviour of effective heat transfer rate in radiating micropolar nanofluid over an expanding sheet with slip effects." *Partial Differential Equations in Applied Mathematics* 11 (2024): 100851. https://doi.org/10.1016/j.padiff.2024.100851
[27] Mishra, S. R., Titilayo M. Agbaje, Rupa Baithalu, and Subhajit Panda. "Spectral quasi-linearization approach for the swimming of motile microorganisms on the bio-convection Casson nanofluid flow over a rotating circular disk." *Numerical Heat Transfer, Part B: Fundamentals* (2024): 1-27. https://doi.org/10.1080/10407790.2024.2352857
[28] Baithalu, Rupa, S. R. Mishra, and Nehad Ali Shah. "Sensitivity analysis of various factors on the micropolar hybrid nanofluid flow with optimized heat transfer rate using response surface methodology: A statistical approach." *Physics of Fluids* 35, no. 10 (2023). https://doi.org/10.1063/5.0171265
[29] Waqas, Hassan, Umar Farooq, Faisal Fareed Bukhari, Metib Alghamdi, and Taseer Muhammad. "Chemically reactive transport of magnetized hybrid nanofluids through Darcian porous medium." *Case Studies in Thermal Engineering* 28 (2021): 101431. https://doi.org/10.1016/j.csite.2021.101431
[30] Venkateswarlu, B., Santosh Chavan, Sang Woo Joo, and Sung Chul Kim. "Entropy analysis of electromagnetic trihybrid nanofluid flow with temperature-dependent viscosity in a Darcy-Forchheimer porous medium over a stretching sheet under convective conditions." *Journal of Molecular Liquids* 393 (2024): 123660. https://doi.org/10.1016/j.molliq.2023.123660
[31] Nazir, Umar, M. Adil Sadiq, and M. Nawaz. "Non-Fourier thermal and mass transport in hybridnano-Williamson fluid under chemical reaction in Forchheimer porous medium." *International Communications in Heat and Mass Transfer* 127 (2021): 105536. https://doi.org/10.1016/j.icheatmasstransfer.2021.105536
[32] Mebarek-Oudina, Fateh, Ines Chabani, Hanumesh Vaidya, and Abdul Aziz I. Ismail. "Hybrid-nanofluid magneto-convective flow and porous media contribution to entropy generation." *International Journal of Numerical Methods for Heat & Fluid Flow* 34, no. 2 (2024): 809-836. https://doi.org/10.1108/HFF-06-2023-0326
[33] Rashad, Ahmed M., Mohamed A. Nafe, and Dalia A. Eisa. "Heat variation on MHD Williamson hybrid nanofluid flow with convective boundary condition and Ohmic heating in a porous material." *Scientific Reports* 13, no. 1 (2023): 6071. https://doi.org/10.1038/s41598-023-33043-z
[34] Rawat, Sawan Kumar, Moh Yaseen, Umair Khan, Manoj Kumar, Sayed M. Eldin, Abeer M. Alotaibi, and Ahmed M. Galal. "Significance of non-uniform heat source/sink and cattaneo-christov model on hybrid nanofluid flow in a Darcy-forchheimer porous medium between two parallel rotating disks." *Frontiers in Materials* 9 (2023): 1097057. https://doi.org/10.3389/fmats.2022.1097057
[35] Asghar, Adnan, Sumera Dero, Liaquat Ali Lund, Zahir Shah, Mansoor H. Alshehri, and Narcisa Vrinceanu. "Slip effects on magnetized radiatively hybridized ferrofluid flow with acute magnetic force over shrinking/stretching surface." *Open Physics* 22, no. 1 (2024): 20240052. https://doi.org/10.1515/phys-2024-0052

[36] Farooq, Umer, Musawara Safeer, Jifeng Cui, Muzamil Hussain, and Nitasha Naheed. "Forced convection analysis of Williamson-based magnetized hybrid nanofluid flow through a porous medium: Nonsimilar modeling." *Numerical Heat Transfer, Part B: Fundamentals* (2024): 1-17. https://doi.org/10.1080/10407790.2023.2300704

[37] Lund, Liaquat Ali, Adnan Asghar, Ghulam Rasool, and Ubaidullah Yashkun. "Magnetized casson SA-hybrid nanofluid flow over a permeable moving surface with thermal radiation and Joule heating effect." *Case Studies in Thermal Engineering* 50 (2023): 103510.

[38] Pop, Ioan, Teodor Groșan, Cornelia Revnic, and Alin V. Roșca. "Unsteady flow and heat transfer of nanofluids, hybrid nanofluids, micropolar fluids and porous media: A review." *Thermal Science and Engineering Progress* 46 (2023): 102248. https://doi.org/10.1016/j.tsep.2023.102248

[39] Rasool, Ghulam, Wang Xinhua, Liaquat Ali Lund, Ubaidullah Yashkun, Abderrahim Wakif, and Adnan Asghar. "Dual solutions of unsteady flow of copper-alumina/water based hybrid nanofluid with acute magnetic force and slip condition." *Heliyon* 9, no. 12 (2023). https://doi.org/10.1016/j.heliyon.2023.e22737

[40] Sayed, Hamed M., Emad H. Aly, and K. Vajravelu. "Influence of slip and convective boundary conditions on peristaltic transport of non-Newtonian nanofluids in an inclined asymmetric channel." *Alexandria Engineering Journal* 55, no. 3 (2016): 2209-2220. https://doi.org/10.1016/j.aej.2016.04.041

[41] Aziz, Abdul. "A similarity solution for laminar thermal boundary layer over a flat plate with a convective surface boundary condition." *Communications in Nonlinear Science and Numerical Simulation* 14, no. 4 (2009): 1064-1068. https://doi.org/10.1016/j.cnsns.2008.05.003

[42] Aly, Emad H., and Ioan Pop. "MHD flow and heat transfer over a permeable stretching/shrinking sheet in a hybrid nanofluid with a convective boundary condition." *International Journal of Numerical Methods for Heat & Fluid Flow* 29, no. 9 (2019): 3012-3038. https://doi.org/10.1108/HFF-12-2018-0794

[43] Asghar, Adnan, Narcisa Vrinceanu, Teh Yuan Ying, Liaquat Ali Lund, Zahir Shah, and Vineet Tirth. "Dual solutions of convective rotating flow of three-dimensional hybrid nanofluid across the linear stretching/shrinking sheet." *Alexandria Engineering Journal* 75 (2023): 297-312. https://doi.org/10.1016/j.aej.2023.05.089

[44] Khashi'ie, Najiyah Safwa, Norihan Md Arifin, Ioan Pop, Roslinda Nazar, Ezad Hafidz Hafidzuddin, and Nadihah Wahi. "Three-dimensional hybrid nanofluid flow and heat transfer past a permeable stretching/shrinking sheet with velocity slip and convective condition." *Chinese Journal of Physics* 66 (2020): 157-171. https://doi.org/10.1016/j.cjph.2020.03.032

[45] Yahaya, Rusya Iryanti, Norihan Md Arifin, Ioan Pop, Fadzilah Md Ali, and Siti Suzilliana Putri Mohamed Isa. "Dual solutions for MHD hybrid nanofluid stagnation point flow due to a radially shrinking disk with convective boundary condition." *International Journal of Numerical Methods for Heat & Fluid Flow* 33, no. 2 (2023): 456-476. https://doi.org/10.1108/HFF-05-2022-0301

[46] Waini, I., A. Ishak, and I. Pop. "Hybrid nanofluid flow and heat transfer past a permeable stretching/shrinking surface with a convective boundary condition." In *Journal of Physics: Conference Series*, vol. 1366, no. 1, p. 012022. IOP Publishing, 2019. https://doi.org/10.1088/1742-6596/1366/1/012022

[47] Asghar, Adnan, Yuan Ying Teh, Muhammad Javed Iqbal, and Liaqat Ali. "Thermal characterization of hybrid nanofluid with impact of convective boundary layer flow and Joule heating law: Dual solutions case study." *Modern Physics Letters B* 38, no. 19 (2024): 2450158. https://doi.org/10.1142/S0217984924501586

[48] Francis, P., P. Sambath, U. Fernandez-Gamiz, S. Noeiaghdam, and S. Dinarvand. "Computational analysis of bio-convective eyring-powell nanofluid flow with magneto-hydrodynamic effects over an isothermal cone surface with convective boundary condition." *Heliyon* 10, no. 3 (2024). https://doi.org/10.1016/j.heliyon.2024.e25088

[49] Khan, Sami Ullah, Aaqib Majeed, and Sakeena Aziz. "Thermal prediction of rotatory multiwall carbon nanotubes subject to convective boundary conditions and slip effects: Implicit finite difference simulations." *Numerical Heat Transfer, Part B: Fundamentals* (2024): 1-14. https://doi.org/10.1080/10407790.2024.2306274

[50] Hayat, Tanzila, and S. Nadeem. "Heat transfer enhancement with Ag–CuO/water hybrid nanofluid." *Results in physics* 7 (2017): 2317-2324. https://doi.org/10.1016/j.rinp.2017.06.034

[51] Zainal, Nurul Amira, Roslinda Nazar, Kohilavani Naganthran, and Ioan Pop. "Heat generation/absorption effect on MHD flow of hybrid nanofluid over bidirectional exponential stretching/shrinking sheet." *Chinese Journal of Physics* 69 (2021): 118-133. https://doi.org/10.1016/j.cjph.2020.12.002

[52] Wahid, Nur Syahirah, Norihan Md Arifin, Najiyah Safwa Khashi'ie, and Ioan Pop. "Hybrid nanofluid slip flow over an exponentially stretching/shrinking permeable sheet with heat generation." *Mathematics* 9, no. 1 (2020): 30. https://doi.org/10.3390/math9010030

[53] Ahmad, Hijaz, Abeer S. Alnahdi, Muhammad Bilal, Muhammad Daher Albalwi, and Abdullah A. Faqihi. "Energy and mass transmission through hybrid nanofluid flow passing over a spinning sphere with magnetic effect and heat source/sink." *Nanotechnology Reviews* 13, no. 1 (2024): 20230194. https://doi.org/10.1515/ntrev-2023-0194

[54] Fadhel, Mustafa Abbas, Adnan Asghar, Liaquat Ali Lund, Zahir Shah, Narcisa Vrinceanu, and Vineet Tirth. "Dual numerical solutions of Casson SA–hybrid nanofluid toward a stagnation point flow over stretching/shrinking cylinder." *Nanotechnology Reviews* 13, no. 1 (2024): 20230191. https://doi.org/10.1515/ntrev-2023-0191

[55] Sharma, Ram Prakash, and Kirnu Badak. "Heat transport of radiative ternary hybrid nanofluid over a convective stretching sheet with induced magnetic field and heat source/sink." *Journal of Thermal Analysis and Calorimetry* 149, no. 9 (2024): 3877-3889. https://doi.org/10.1007/s10973-024-12979-y

[56] Soomro, Azhar Mustafa, Liaquat Ali Lund, Adnan Asghar, Ebenezer Bonyah, Zahir Shah, and Hakim AL Garalleh. "Magnetized Casson SA-hybrid nanofluid flow over a permeable moving surface with stability analysis." *International Journal of Thermofluids* 21 (2024): 100555. https://doi.org/10.1016/j.ijft.2023.100555

[57] Waini, Iskandar, Anuar Ishak, and Ioan Pop. "Hybrid nanofluid flow induced by an exponentially shrinking sheet." *Chinese Journal of Physics* 68 (2020): 468-482. https://doi.org/10.1016/j.cjph.2019.12.015

[58] Ghosh, Sudipta, and Swati Mukhopadhyay. "Stability analysis for model-based study of nanofluid flow over an exponentially shrinking permeable sheet in presence of slip." *Neural Computing and Applications* 32, no. 11 (2020): 7201-7211. https://doi.org/10.1007/s00521-019-04221-w